SUPPORTING INFORMATION

^{1}H and ^{13}C hyperfine coupling constants of the tryptophanyl cation radical in aqueous solution from microsecond time-resolved CIDNP

Alexey S. Kiryutin, Olga B. Morozova, Lars T. Kuhn,

Alexandra V. Yurkovskaya and P. J. Hore

S1. Complete reference 48.

M. J. Frisch; G. W. Trucks; H. B. Schlegel; G. E. Scuseria; M. A. Robb; J. R. Cheeseman; J. A. Montgomery; Jr., T. V.; K. N. Kudin; J. C. Burant; J. M. Millam; S. S. Iyengar; J. Tomasi; V. Barone; B. Mennucci; M. Cossi; G. Scalmani; N. Rega; G. A. Petersson; H. Nakatsuji; M. Hada; M. Ehara; K. Toyota; R. Fukuda; J. Hasegawa; M. Ishida; T. Nakajima; Y. Honda; O. Kitao; H. Nakai; M. Klene; X. Li; J. E. Knox; H. P. Hratchian; J. B. Cross; C. Adamo; J. Jaramillo; R. Gomperts; R. E. Stratmann; O. Yazyev; A. J. Austin; R. Cammi; C. Pomelli; J. W. Ochterski; P. Y. Ayala; K. Morokuma; G. A. Voth; P. Salvador; J. J. Dannenberg; V. G. Zakrzewski; S. Dapprich; A. D. Daniels; M. C. Strain; O. Farkas; D. K. Malick; A. D. Rabuck; K. Raghavachari; J. B. Foresman; J. V. Ortiz; Q. Cui; A. G. Baboul; S. Clifford; J. Cioslowski; B. B. Stefanov; G. Liu; A. Liashenko; P. Piskorz; I. Komaromi; R. L. Martin; D. J. Fox; T. Keith; M. A. Al-Laham; C. Y. Peng; A. Nanayakkara; M. Challacombe; P. M. W. Gill; B. Johnson; W. Chen; M. W. Wong; C. Gonzalez; Pople, J. A. *Gaussian 03, Revision D.02*, 2004.

S2. NMR parameters used for spectral simulations

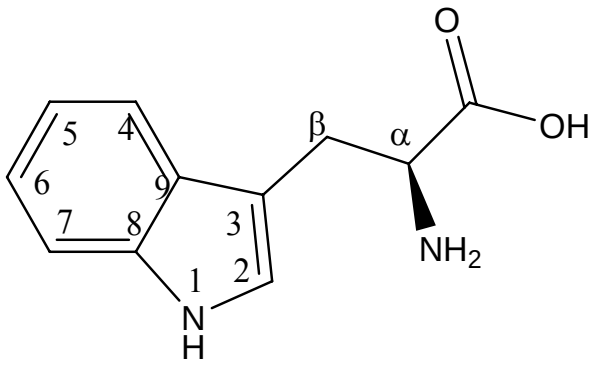

Chart S2.1. Numbering scheme for tryptophan.

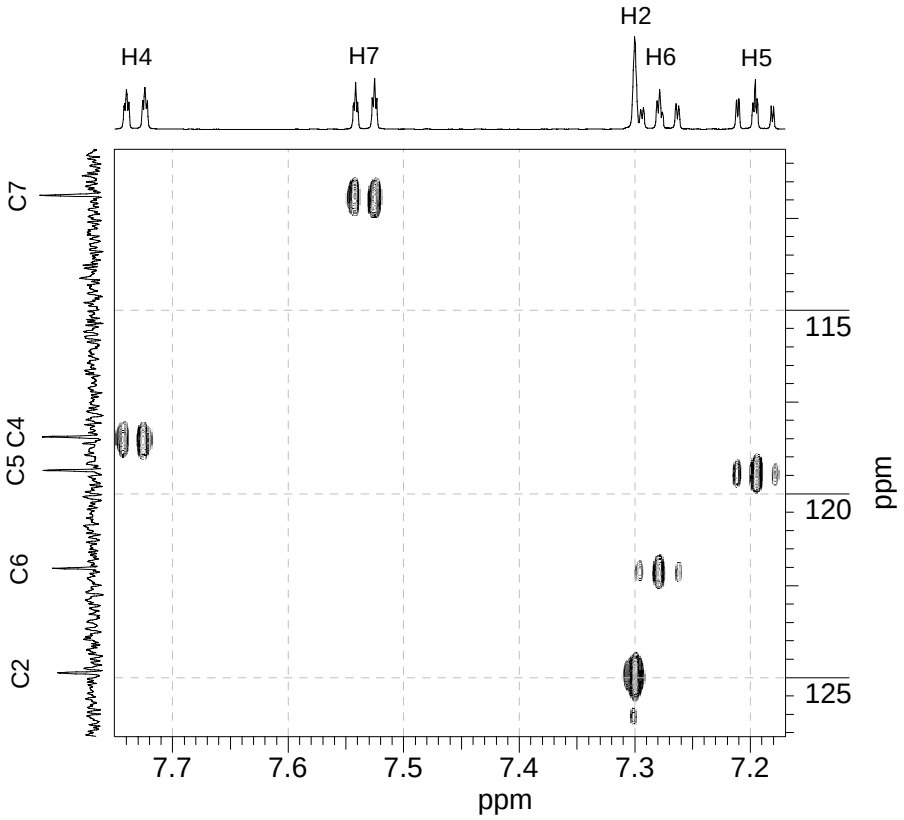

Figure S2.1. Aromatic region of the HMQC spectrum of tryptophan (natural isotopic abundance) in D_2O. [Trp] = 50 mM, pH = 9.0.

Table S2.1. ^{13}C NMR parameters of tryptophan.

Carbon	Chemical shift / ppm	J_{CC} / Hz	$^{1}J_{CH}$ / Hz	Linewidth / Hz
CO	174.62	54.2 (Cα); 3.0 (Cβ)	n/a	3
Cα	55.01	54.2 (CO); 3.0 (Cβ); 5.0 (C2)	145	5
Cβ	26.36	3.0 (CO); 3.0 (Cα); 1.0 (C2); 51.0 (C3)	130; 130	6
C2	124.92	5.0 (Cα); 1.0 (Cβ), 70.0 (C3); 3.0 (C8); 5.1 (C9)	181	20
C3	107.42	51.0 (Cβ), 70.0(C2); 1.0 (C4); 51.0 (C9)	n/a	8
C4	118.35	1.0 (C3); 59.4 (C5); 5.4 (C6); 3.1 (C8); 55.5 (C9)	158	3
C5	119.35	59.4 (C4); 57.0 (C6); 3.1 (C7); 3.0 (C9)	158	3
C6	122.03	5.4 (C4); 57.0 (C5); 59.5 (C7); 2.8 (C8)	159	3
C7	111.82	3.1 (C5); 59.5 (C6); 64.0 (C8); 1.0 (C9)	162	8
C8	136.25	3.0 (C2); 2.8 (C6); 61.3 (C9)	n/a	20
C9	126.55	5.1 (C2); 51.0 (C3); 55.5 (C4); 3.0 (C5); 1.0 (C7); 61.3 (C9)	n/a	4

Table S2.2. ^{1}H NMR parameters of tryptophan.

Proton	Chemical shift / ppm	J_{HH} / Hz	Linewidth / Hz
Hα	4.62	7.7 (Hβ1); 5.3 (Hβ2)	2
Hβ1	3.17	7.7 (Hα); 14.7 (Hβ2)	2
Hβ2	3.29	5.3 (Hα); 14.7 (Hβ1)	2
H2	7.19	0.5 (Hβ1); 0.7 (Hβ2)	2
H4	7.60	8.0 (H5); 1.1 (H6); 0.8 (H7)	2
H5	7.09	8.0 (H4); 7.1 (H6); 1.0 (H7)	2
H6	7.18	1.1 (H4); 7.1 (H5); 8.26 (H7)	2
H7	7.39	0.8 (H4); 1.0 (H5); 8.26 (H6)	2

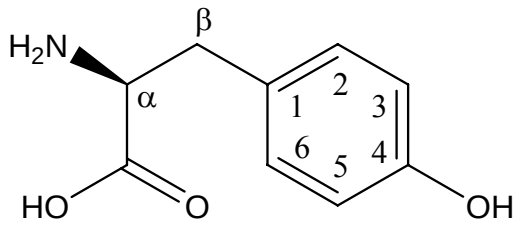

Chart S2.2. Numbering scheme for tyrosine.

Table S2.3. ^{13}C NMR parameters of tyrosine**.**

Carbon	Chemical shift / ppm	J_{CC} / Hz	$^{1}J_{CH}$ / Hz	Linewidth / Hz
CO	182.42	53.1 (Cα)	n/a	10
Cα	58.28	53.1 (CO); 34.0 (Cβ)	140.8	12
Cβ	40.05	34.0 (Cα); 45.0 (C1)	129.0; 129.0	12
C2,C6	131.61	57.0 (C1); 58.1 (C3,C5)	155.4	15
C3,C5	118.49	58.1 (C2,C6); 64.8 (C4)	155.3	15
C4	162.02	64.0 (C3,C5)	n/a	20

Table S2.4. ^{1}H NMR parameters of tyrosine.

Proton	Chemical shift / ppm	J_{HH} / Hz	Linewidth / Hz
Hα	3.36	5.0 (Hβ1); 7.6 (Hβ2)	2
Hβ1	2.78	5.0 (Hα); 13.6 (Hβ2)	2
Hβ2	2.56	7.6 (Hα); 13.6 (Hβ1)	2
H2	6.91	8.3 (H3); 0.3 (H5); 2.6 (H6)	2
H3	6.49	8.3 (H2); 2.6 (H5); 0.3 (H6)	2
H5	6.49	0.3 (H2); 2.6 (H3); 8.3 (H6)	2
H6	6.91	2.6 (H2); 0.3 (H3); 8.3 (H5)	2

S3. EPR parameters of FMN anion radical.

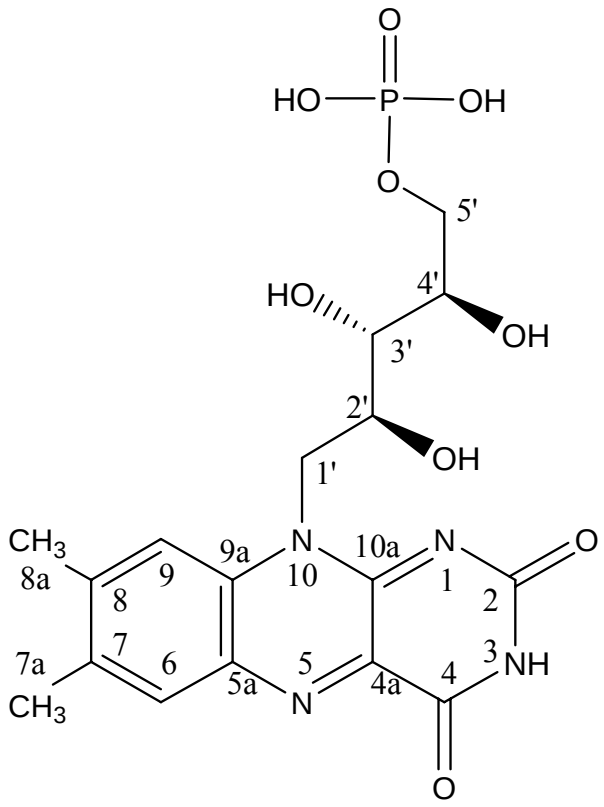

Chart S3. Numbering scheme for FMN.

Table S3. Isotropic hyperfine coupling constants of FMN anion radical (g = 2.0034)

Atom	H6	8a-CH_3	N5	N10
HFC / G	–3.5	4.0	7.3	3.1

S4. EPR parameters of DP radical

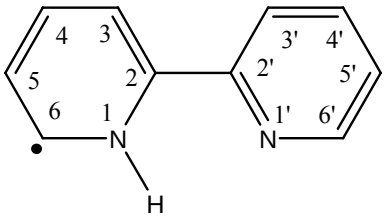

Chart S4. Numbering scheme for DP radical.

Table S4. Isotropic hyperfine constants of DP radical (g = 2.0030) from Ref. 45.

Atom	N1	N1′	H1	H3	H4	H5	H6	H3′	H4′	H5′	H6′
HFC / G	4.07	2.26	–6.79	2.16	–7.56	–1.9	–2.12	–2.4	0.3	–4.19	1.12

S5. Calculated hyperfine coupling constants

The following tables contain the isotropic hyperfine coupling constants for $TrpH^{\bullet+}$, $Trp^{\bullet}$, $TyrH^{\bullet+}$ and $Tyr^{\bullet}$ radicals calculated using Gaussian 03[48] as described in the Experimental Methods.

Table S5.1. Isotropic HFCs of tryptophan radicals (Gauss)

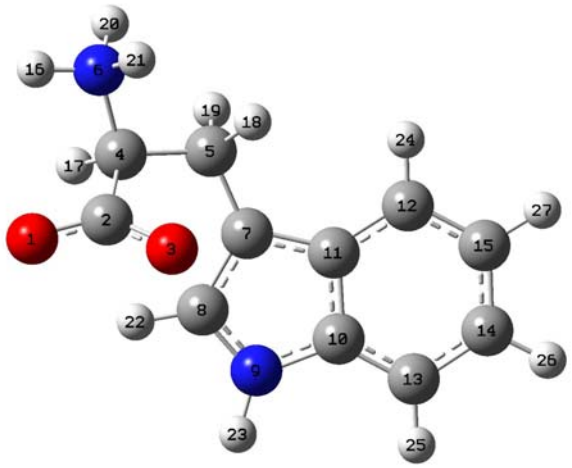

Numbering scheme for tryptophan radicals

No.	Atom	$TrpH^{\bullet+}$ in water	$Trp^{\bullet}$ in water	$TrpH^{\bullet+}$ in vacuo	$Trp^{\bullet}$ in vacuo
1	O(17)	–0.19821	–0.09127	–0.00759	–0.22446
2	C(13)	–0.44882	–0.18455	0.26679	1.12086
3	O(17)	–3.01849	–1.06496	–1.15541	–0.20875
4	C(13)	0.25458	0.58631	0.08111	12.16675
5	C(13)	–5.12333	–6.40715	–3.56810	–6.10740
6	N(14)	–0.11126	–0.12197	1.46482	0.12510
7	C(13)	12.54413	16.89637	6.29336	16.17951
8	C(13)	–2.27426	–8.30377	–2.80031	–9.18212
9	N(14)	1.94959	3.33034	3.21532	3.71344
10	C(13)	0.92156	0.20761	–3.59447	–0.36018
11	C(13)	–8.90588	–9.53185	–5.45310	–8.59758

12	C(13)	6.19106	5.44432	4.75255	5.06488
13	C(13)	–1.82162	–2.00506	2.89974	–1.53204
14	C(13)	4.42705	3.82754	0.32448	3.40005
15	C(13)	–4.98694	–4.23261	–2.32869	–3.79639
16	H(1)	0.09376	0.00203	–0.39640	–0.03468
17	H(1)	0.01499	–0.09344	–0.93072	–0.84602
18	H(1)	11.88845	15.42452	16.04575	13.77962
19	H(1)	25.43966	27.86591	0.45698	3.31798
20	H(1)	0.01547	–0.00972	–0.10390	0.04785
21	H(1)	0.02070	0.04669	0.23313	0.24329
22	H(1)	–4.21250	–0.53025	–2.78016	0.48438
23	H(1)	–4.13008	–	–5.98344	–
24	H(1)	–5.03693	–4.47454	–4.88005	–4.37214
25	H(1)	–0.50332	–0.34469	–3.63695	–0.56995
26	H(1)	–4.12289	–3.68296	–2.08282	–3.56047
27	H(1)	1.23537	0.79050	–0.40011	0.64307

Table S5.2. Isotropic HFCs of tyrosine radicals (Gauss)

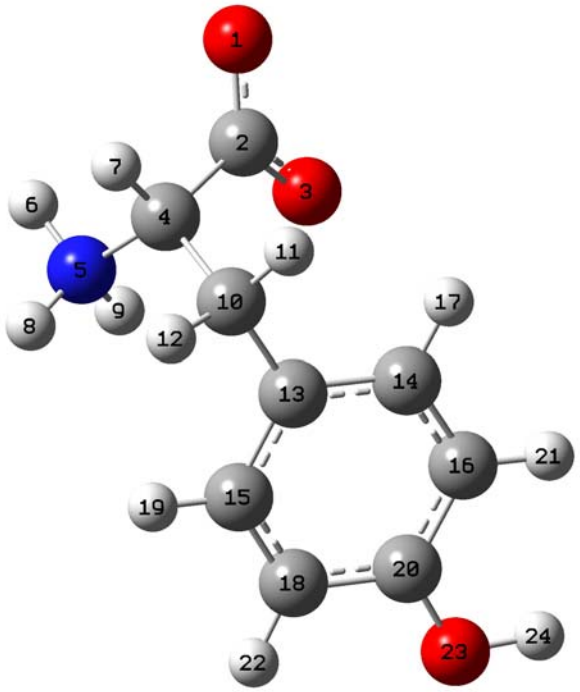

Numbering scheme for tyrosine radicals

No.	Atom	$TyrOH^{\bullet+}$ in water	$TyrO^{\bullet}$ in water	$TyrOH^{\bullet+}$ in vacuo	$TyrO^{\bullet}$ in vacuo
1	O(17)	–0.32620	–0.24552	0.36727	–0.27801
2	C(13)	–0.52304	–0.33128	3.09290	–0.23421
3	O(17)	–1.08562	–0.38620	–2.38671	–0.01317
4	C(13)	6.77639	7.39030	–1.13691	10.52017
5	N(14)	–0.13522	–0.09744	2.61513	–0.26964
6	H(1)	0.21729	0.00132	–0.95544	–0.09556
7	H(1)	–0.51050	–0.25930	–0.83576	0.09017
8	H(1)	0.32133	0.17359	–0.78399	0.03712
9	H(1)	0.01240	0.00224	–0.75244	–0.10293
10	C(13)	–5.14158	–4.91629	–4.21843	–4.47071
11	H(1)	7.11054	5.20028	22.05441	5.90809
12	H(1)	7.88897	7.24854	–0.62087	4.96242
13	C(13)	12.43229	13.00725	6.40789	12.43122
14	C(13)	–5.71168	–8.04060	–1.81809	–8.55851

15	C(13)	–7.07102	–8.57445	–3.75328	–8.56598
16	C(13)	1.84114	5.49537	–1.24100	7.25563
17	H(1)	0.36931	1.97217	–1.35957	2.56399
18	C(13)	3.60629	6.38732	0.64728	7.24672
19	H(1)	1.06096	2.09080	–0.23392	2.60492
20	C(13)	–2.03724	–8.84836	1.91853	–11.79721
21	H(1)	–3.82070	–5.79828	–1.53052	–6.81549
22	H(1)	–5.21744	–6.54374	–2.90310	–6.80262
23	O(17)	–7.35915	–8.87973	–4.90735	–9.54570
24	H(1)	–4.35724	–	–3.91050	–

S6. Simulation of CIDNP spectra

In the experiments described here, photo-CIDNP arises from radical pairs created in a spin-correlated triplet state by reaction of the photo-excited dye molecule and an amino acid. Immediate recombination of the radicals, to give the dye and amino acid molecules in their ground states, is impossible until the radical pair has been converted into a singlet state with antiparallel electron spins. This singlet-triplet interconversion, or intersystem crossing, process is driven by the various magnetic interactions enjoyed by the two unpaired electrons, namely the difference in their Zeeman interactions with the strong static field B_0, and the intramolecular hyperfine couplings to magnetic nuclei. In a field much stronger than the hyperfine interactions, only the singlet (S) and $m_S = 0$ triplet (T_0) states of the pair are involved; they interconvert coherently at a frequency equal to half the difference in Larmor frequencies of the two electron spins. For a radical pair with a single spin-½ nucleus, this frequency is

$$\omega(m_I) = \Delta g \mu_B B_0 / \hbar + m_I a \qquad (1)$$

where m_I is the magnetic quantum number of the nucleus ($m_I = \pm ½$), a is the hyperfine coupling constant and Δg is the difference in the g-values of the two radicals. For typical values of Δg, B_0 and a, singlet-triplet interconversion takes ~1-10 ns, during which time the radicals diffuse and may separate or re-encounter. In the event of a re-encounter the pair may recombine provided it is in a singlet state. Thus, the radical recombination probability depends on whether the nucleus is in its $m_I = +½$ or $–½$ state.

From simple diffusion theory [1], the re-encounter probability at times t greater than ~1 ns after formation of the radical pair is proportional to $t^{-3/2}$, while the singlet probability is proportional to $\sin^2[\omega(m_I)t]$. Integrating over all re-encounter times, and ignoring the possibility of multiple re-encounters, the total recombination probability $P(m_I)$ is proportional to $|\omega(m_I)|^{½}$ [2-4]:

$$P(m_I) \propto \int_0^\infty \sin^2\left[\omega(m_I)t\right] t^{-3/2}\, \mathrm{d}t \propto \left|\omega(m_I)\right|^{1/2} \qquad (2)$$

The polarization of the nucleus in the diamagnetic product of the recombination reaction is therefore proportional to the difference in the recombination probabilities of the m_I = +½ and –½ states:

$$\left|\omega(+\tfrac{1}{2})\right|^{1/2} - \left|\omega(-\tfrac{1}{2})\right|^{1/2} = \left|\Delta g \mu_B B_0 / \hbar + \tfrac{1}{2} a\right|^{1/2} - \left|\Delta g \mu_B B_0 / \hbar - \tfrac{1}{2} a\right|^{1/2} \quad (3)$$

In reality, there are several nuclei in each radical with significant hyperfine interactions. Equations (1) and (3) are easily extended to include as many ^{1}H (spin-½) and ^{14}N (spin-1) nuclei as desired [5].

When $\Delta g \mu_B B_0/\hbar >> ½a$ the polarization is proportional to $a/\Delta g B_0$:

$$\left|\Delta g \mu_B B_0 / \hbar + \tfrac{1}{2} a\right|^{1/2} - \left|\Delta g \mu_B B_0 / \hbar - \tfrac{1}{2} a\right|^{1/2} \approx \left|\frac{\hbar}{\Delta g \mu_B B_0}\right|^{1/2} \frac{a}{2} \quad (4)$$

This simple relation is valid for all weakly coupled nuclei in both tyrosine and tryptophan under the conditions of our experiments, i.e. the polarization of each nucleus in the diamagnetic product is proportional to its hyperfine coupling in the radical precursor and is independent of all other hyperfine couplings. Furthermore, multiplet CIDNP effects (i.e. differential polarization within a spin-spin coupled NMR multiplet) are negligible in this high field limit.

The simulated CIDNP spectra presented in Figures 1, 3, 4 and 5 were obtained from the calculated thermal equilibrium NMR spectra by scaling the signal intensity of each nucleus by the polarization determined as above. The proportionality between the CIDNP intensity and a [Equation (4)] made it particularly straightforward to optimize the agreement between experimental and simulated spectra using the relative hyperfine coupling constants as the fit parameters. The only exception was the pair of strongly coupled carbons (C4 and C5) in tryptophan for which the intensities in the simulated spectra were calculated exactly. For this AB spin system, following [6], we first calculated the relative populations of the Zeeman levels for the two nuclear spins ($P_{\alpha\alpha}$, $P_{\alpha\beta}$, $P_{\beta\alpha}$, $P_{\beta\beta}$) using Adrian's approach and Equation (2) above. The first α or β index refers to C4 and the second to C5. The eigenstates of the AB system are expressed as follows:

$$|1\rangle = |\alpha\alpha\rangle$$
$$|2\rangle = \cos\theta|\alpha\beta\rangle + \sin\theta|\beta\alpha\rangle$$
$$|3\rangle = -\sin\theta|\alpha\beta\rangle + \cos\theta|\beta\alpha\rangle$$
$$|4\rangle = |\beta\beta\rangle \quad (5)$$

so that the eigenstate populations are:

$$P_1 = P_{\alpha\alpha}$$
$$P_2 = P_{\alpha\beta}\cos^2\theta + P_{\beta\alpha}\sin^2\theta$$
$$P_3 = P_{\alpha\beta}\sin^2\theta + P_{\beta\alpha}\cos^2\theta$$
$$P_4 = P_{\beta\beta} \quad (6)$$

The strong-coupling parameter θ, defined by $\theta = \arctan[J/(\omega_4 - \omega_5)]$, is 0.187 radians, where J is the spin-spin coupling constant (59.4 Hz) and ω_4 and ω_5 are the resonance frequencies of the two carbons (see Table S2.1 for the chemical shifts).

All CIDNP spectra were recorded using a 90° flip angle pulse. Using Equation (28) from Ref. [6] we obtain the following expressions for the intensities of the two doublets of the AB system with 90° pulse excitation:

$$I_{AB(1)} = \frac{1}{2}[P_1 + (P_2 - P_3)\cos^2 2\theta - P_4]$$
$$I_{AB(2)} = \frac{1}{2}[P_1 - (P_2 - P_3)\cos^2 2\theta - P_4] \quad (7)$$

In the simulations, we varied the hyperfine coupling constants of C4 and C5 to obtain the best fit of the calculated intensities, $I_{AB(1)}$ and $I_{AB(2)}$, to those observed in the CIDNP spectrum. The small admixture of polarization from C9 and C6 to the C4-C5 multiplet was neglected, but the spin-spin coupling of C4 with C9 and C5 with C6 was included in the spectral simulations.

[1] Noyes, R. M., *J. Chem. Phys.* **1954**, *22*, 1349-1359.

[2] Adrian, F. J., *J. Chem. Phys.* **1970**, *53*, 3374-3375.

[3] Adrian, F. J., *J. Chem. Phys.* **1971**, *54*, 3912-3917.

[4] Kaptein, R., *J. Am. Chem. Soc.,* **1972**, *94*, 6251-6262.

[5] Closs, G. L., *Advances in Magnetic Resonance*, Vol. 7, ed. J. S. Waugh (San Diego: Academic Press) **1974**, pp. 157-229.

[6] Schäublin, S., Höhener, A., and Ernst, R. R., *J. Magn. Reson.* **1974**, *13*, 196-216.